ESSC & DUPLEX 2019

10th European Stainless Steel Conference - Science and Market,
6th European Duplex Stainless Steel Conference & Exhibition

30 September - 02 October 2019
Schönbrunn, Vienna

ASMET
THE AUSTRIAN SOCIETY FOR METALLURGY AND MATERIALS

TU Graz

RODRIGO MAGNABOSCO[1], MARIANA TORTELLA MERLI FIORANTE[1]

THERMO-CALC® AND DICTRA® SIMULATIONS OF THE SOLUTION HEAT TREATMENT OF SUPERDUPLEX STAINLESS STEELS

Abstract

The aim of the present work was to perform computational simulations of the equilibrium and phase transformation kinetics of a superduplex stainless steel UNS S32750 in two different heat treatment cycles: "i" during heating to 1250°C from its initial duplex condition, or "ii" during heating at temperatures to obtain duplex structure from the equilibrium microstructure obtained at 1250°C solution treatment. Thermo-Calc® and DICTRA® simulations were executed, as well as the experimental validation in the laboratory of some of the simulations' results. The experimental validation showed, by quantitative stereology, that equilibrium phase fractions stabilize after 30 min of heat treatment in both thermal cycles, reaching 71% of ferrite in cycle "i" and 51% of austenite in cycle "ii", validating the kinetic simulations concerning phase fractions. However, simulations showed that during heat treatment cycle "i", although ferrite fraction stabilizes in 16 min, chemical elements took 36 min to come into equilibrium in ferrite, and 10h in austenite, indicating that equilibrium is only fully attained long after the phases' fractions stabilize, a fact which the experiments are not able to detect. The geometric model that simulates planar grains and considers the 'reduced composition' is the one that best describes the experimental results.

Keywords

Superduplex Stainless Steel. Heat treatment. Phase transformation. Simulation. DICTRA.

1. Introduction

Superduplex stainless steels (SDSS) are produced for noble applications, including petrochemical, aeronautical and oil and gas sectors, as they combine mechanical strength, toughness and high corrosion resistance, especially the pitting corrosion resistance [1-3]. For SDSS, pitting resistance equivalent number (PREN), defined by Eq. 1, is greater than 40, indicating their potential high pitting corrosion resistance [1,3-5].

$$PREN = wt\ \%Cr + 3.3wt\ \%Mo + 16wt\ \%N \quad (1)$$

Typical microstructure of SDSS is composed by equal volumes of austenite (γ) and ferrite (α) obtained by solution heat treatment between 1000°C and 1300°C, as described in literature [2-3,6], followed by water cooling to keep the duplex structure at room temperature [6].

In this study, simulation of the common thermal condition imposed during forging of a UNS S32750 (SAF 2507) SDSS was conducted, performing heating at 1250°C and evaluating changes in volume fraction of phases in different times. Equivalent analysis was employed simulating the solution-treatment of an alloy that was prior subjected to heating for 3 h at 1250 °C, studying the changes in ferrite-to-austenite volume fraction at a temperature where

[1] FEI UNIVERSITY

the duplex structure can be formed. Thermo-Calc® simulations were used to determine equilibrium conditions in different temperatures for the alloy, and DICTRA® simulations were used to evaluate the kinetics of austenite-to-ferrite or ferrite-to-austenite transformations [7-8]. Verification of the validity of the computer simulations was carried out with laboratory experiments.

2. Computational Modelling

Computational modelling was done for two different heat cycles. Cycle "i" simulated the thermal condition imposed during forging, which basically is the heating to 1250°C of a typical duplex microstructure, and cycle "ii", which simulated the necessary solution-treatment to develop the duplex structure after the previous forging cycle "i".

To determine the solution-treatment temperature which allow the formation of 50% of ferrite and 50% of austenite, thermodynamic phases' equilibrium was obtained throughout Thermo-Calc® version 2018b, using TCFE8 database, for two different chemical compositions of the UNS S32750 steel: one is the complete composition, as shown in Table 1, and the other is called "reduced composition", that is, only with the main elements of interest, Cr, Ni, Mo, N and Fe.

Table 1 – UNS S32750 complete chemical composition (wt %)

Cr	Ni	Mo	N	Mn	W	C	Fe
25.17	6.88	3.61	0.25	0.60	0.69	0.01	balance

Considering the results of both simulations, it was noticed that the differences between simulations using the complete or the reduced chemical compositions are minimal. For this reason, only the reduced chemical composition was used in computer simulations, saving simulation time in the kinetics simulations using DICTRA®. It was found that 1088 °C is the solution-treatment temperature to develop the duplex structure. For simulating forging conditions, 1250 °C was chosen as the temperature during a typical hot working.

DICTRA® simulations, using TCFE8 and MOBFE3 databases, were performed to simulate planar or spherical geometric models of the microstructure, to define which one better describes the experimental results conducted for validation. Geometric models are shown in Fig. 1. In planar model (Fig. 1a), the phases' lengths were estimated considering the average grain size of the phases measured by optical metallography and respecting the volumetric fraction of phases determined in Thermo-Calc® simulation for the initial condition of the simulation model. Spherical model consider as phases' lengths the austenite medium grain radius with a spherical ferrite shell since ferrite is usually described as the matrix phase in SDSS. The grain sizes were calculated by the method of the linear intercepts in optical micrographs obtained after metallographic preparation and electrolytic etching in 10% oxalic acid solution under 6 Vcc for 30 s.

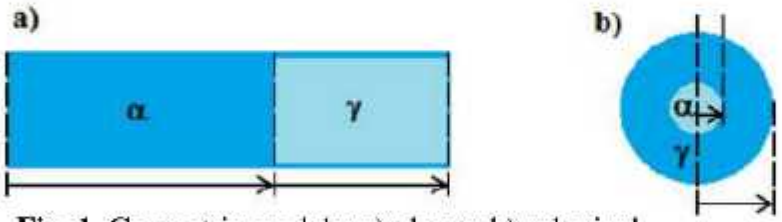

Fig. 1. Geometric models: a) planar; b) spherical.

Before cycle "i", the material in the supplied condition was in thermodynamic equilibrium, since it was treated at 1120 °C for 1 h and 30 min and immediately water cooled, were the system reached the balance of ferrite and austenite fractions of 49:51, respectively. The real phase fractions were used as parameters for the simulations, which phase with a determined chemical composition in Thermo-Calc®.

Before cycle "ii", considering that the material was heat-treated at 1250 °C for 3 h and the system reached a balance of ferrite and austenite fractions of 70:30, respectively, the simulations also considered as chemical composition of such phases the ones determined in Thermo-Calc® simulations for equilibrium at 1250 °C

For each model, the simulations took approximately 10h to complete, using a computer with Intel® Core ™ i7-4770 CPU @ 3.40 GHz and 8 cores.

The parameters used for the forging and solution-treatment to duplex structure simulations can be seen in Table 2 and Table 3, respectively.

Table 2 – Parameters used in heat cycle "i" simulation.

Simulation time	Temperature	Geometric model	α length	γ length
3 h	1250 °C	Planar	10 μm	10 μm
16 h	1250 °C	Spherical	1.3 μm	5 μm

Table 3 – Parameters used in heat cycle "ii" simulation.

Simulation time	Temperature	Geometric model	α length	γ length
1000 h	1088 °C	Planar	67 μm	28 μm
20 h	1088 °C	Spherical	6.9 μm	14 μm

3. Experimental procedures

Isothermal heat treatments were conducted at both thermal cycles for different times, described in the Table 4. Samples treated in cycle "ii" were pre-treated at 1250 °C for 3 h and water quenched.

Table 4 – Heat treatments realized

Thermal cycle	Temperature	Time
i	1250 °C	1 min, 2 min, 40 min, 3 h
ii	1088 °C	2 min, 30 min, 3 h, 12 h, 36 h

Metallographic specimens of all heat-treated samples were prepared to be analysed under optical microscopy, using the modified Beraha reagent, which promotes selective etching of phases, and using electrolytic etching with oxalic acid, aiming to reveal grain boundaries, allowing the measurement of its mean size, following the method of linear intercepts.

Stereological quantitative analysis for determination of ferrite and austenite volume fractions was performed using optical microscopy images of the Beraha etched specimens, using Olympus AnalySIS docu software, performing measurements in 20 random fields at 100 times magnification.

4. Results and discussion

Equilibrium simulation using Thermo-Calc® defined the solution-treatment temperature of 1088 °C to reach the SDSS initial duplex condition, achieving 50% of austenite and 50% of ferrite, as shown in Fig. 2. In the chosen temperature for simulation of the forging conditions, 1250 °C, the microstructure is estimated to have 30% of austenite and 70% of ferrite.

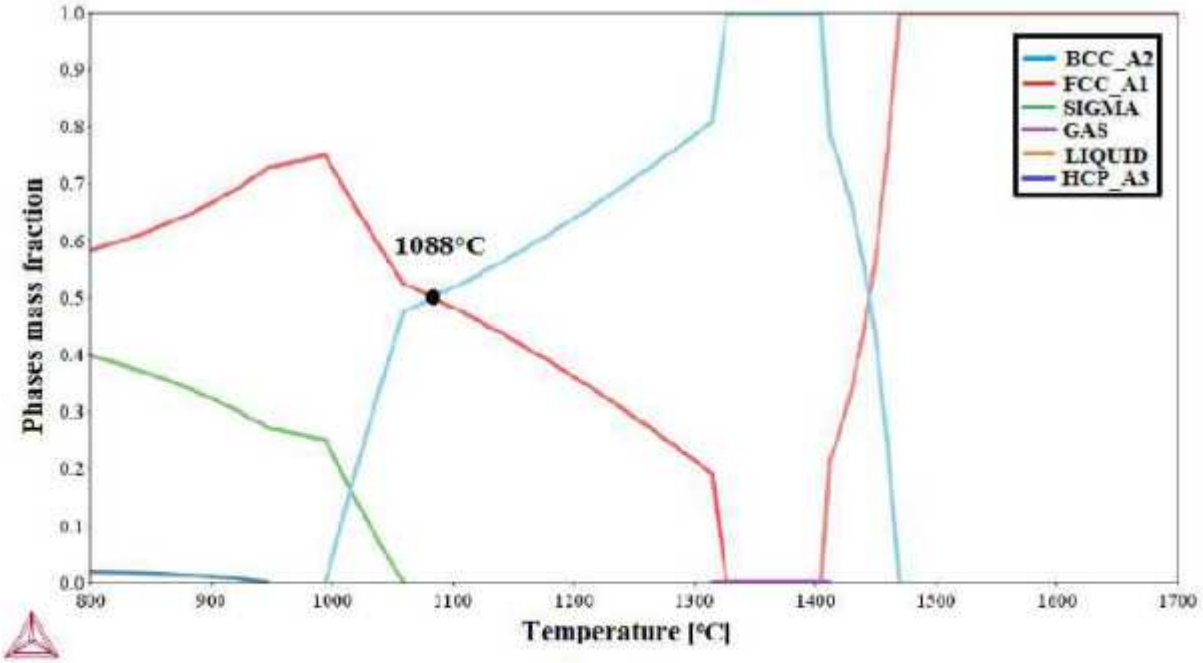

Fig. 2. Equilibrium diagram as a function of temperature for the studied SDSS. TCFE8 database

Microstructures formed in samples after thermal cycles "i" or "ii" at different times are presented in Fig. 3 and Fig. 4. A typical SDSS microstructure can be observed, with a ferritic matrix in dark color, and the austenitic phase in the light color.

Heating at 1250 °C for 1 min (Fig. 3a), lead to only smaller grains and balanced amounts of both phases, whereas between 2 min and 40 min (Fig. 3b and 3c, respectively) the ferrite volume fraction increased. Analysis by stereological quantitative confirms the evolution of the ferritic phase observed in the micrographs, showing that the equilibrium is reached after 30 min (1800 s) of heat treatment, with 71% ± 2.5% of ferrite, as shown by the experimental points in Fig. 5. The sample treated at 1250 °C for 3 h (Fig. 3b) was used as reference of equilibrium at 1250 °C, and the mean size of grains was used as the length of phases in DICTRA® simulations of the cycle "ii", as shown in Table 3.

Sample heated at 1088 °C during 2 min (Fig. 4a) presented only small amounts of austenite, whereas after 30 min (Fig. 4b) the volume fraction of austenite increased and remain practically constant up to 36 h of heat treatment (Fig. 4c and 4d), indicating that equilibrium was reached in this time frame. It is also observed that at 3 h of heat treatment

(Fig. 4c) there is nucleation of austenite inside the ferrite's grains, which cannot be implemented in the geometry of the simulation models. For longer times (Fig. 4d), coalescence of austenite is observed. Quantitative volume fraction of phases (experimental dots in Fig. 6) showed that thermodynamic equilibrium of volume fraction of phases at 1088 °C is also reached after 30 min (1800 s) of heat treatment, resulting in 51% ± 2.2 % of austenite.

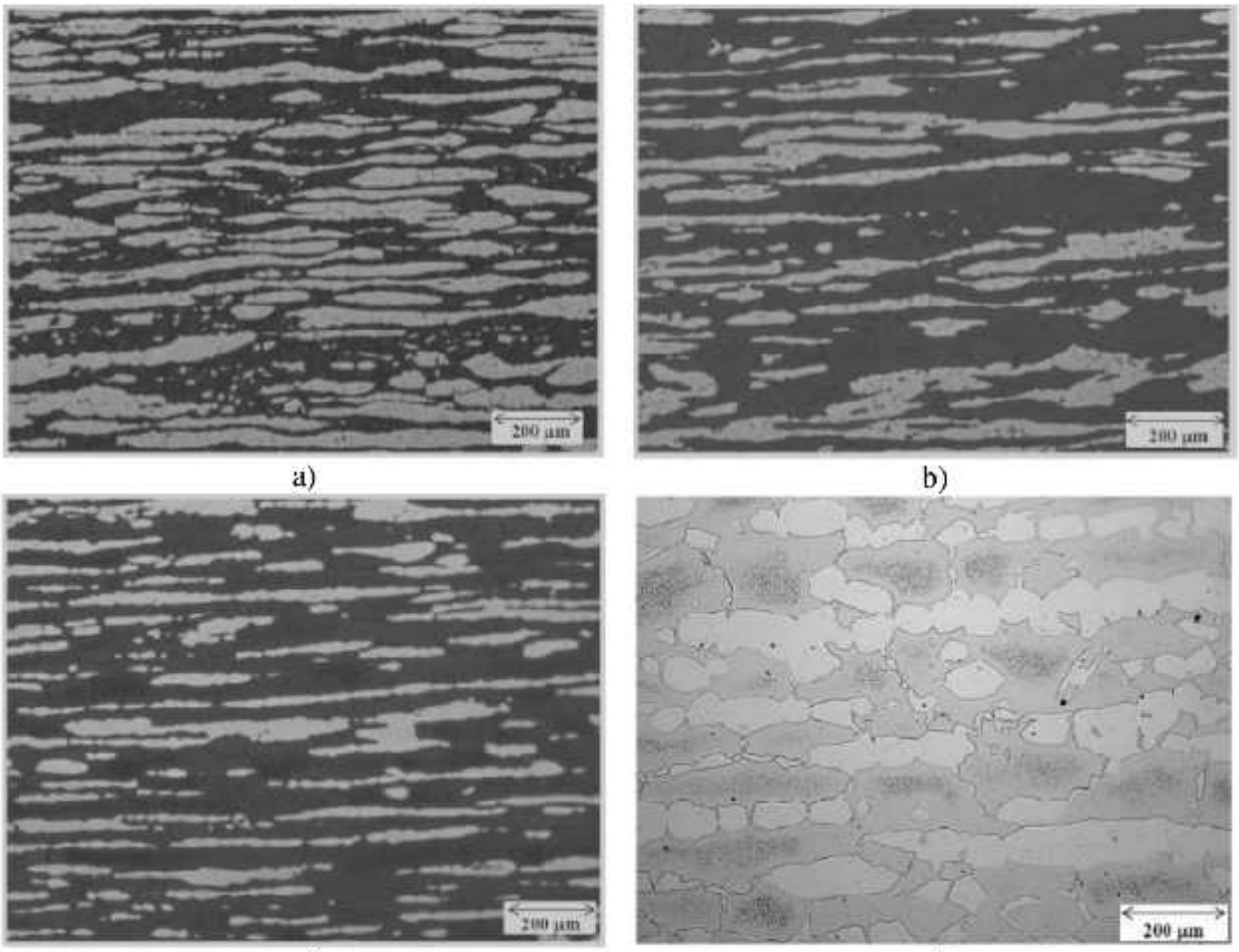

Fig. 3. Optical microscopy of the samples solubilized at 1250 °C for different times, etched with modified Beraha in a) 1 min, b) 2 min, c) 40 min and electrolytic etched with oxalic acid in d) 3 h.

The volume fractions of phase's evolution are presented in Fig. 5 and Fig. 6 for the two heat cycles, comparing DICTRA models to the experimental results, with an expected sigmoidal behaviour [9]. It was shown that the planar geometry model does not describe the experimental results obtained in cycle "i" (Fig. 5), except at equilibrium, when it reaches the expected ferrite fraction, 71%. However, the planar model for cycle "ii" (Fig. 6) describes the experimental results, reaching the measured austenite fraction during all treatment time. Moreover, the spherical geometry grains model is only able to describe the experimental results of cycle "ii" (Fig. 6) after 30 min, since the curve overlaps the planar one. Thus, none of the geometric grain models are able to exactly describe heat cycles, however, the planar geometry is the one closest to the experiments results.

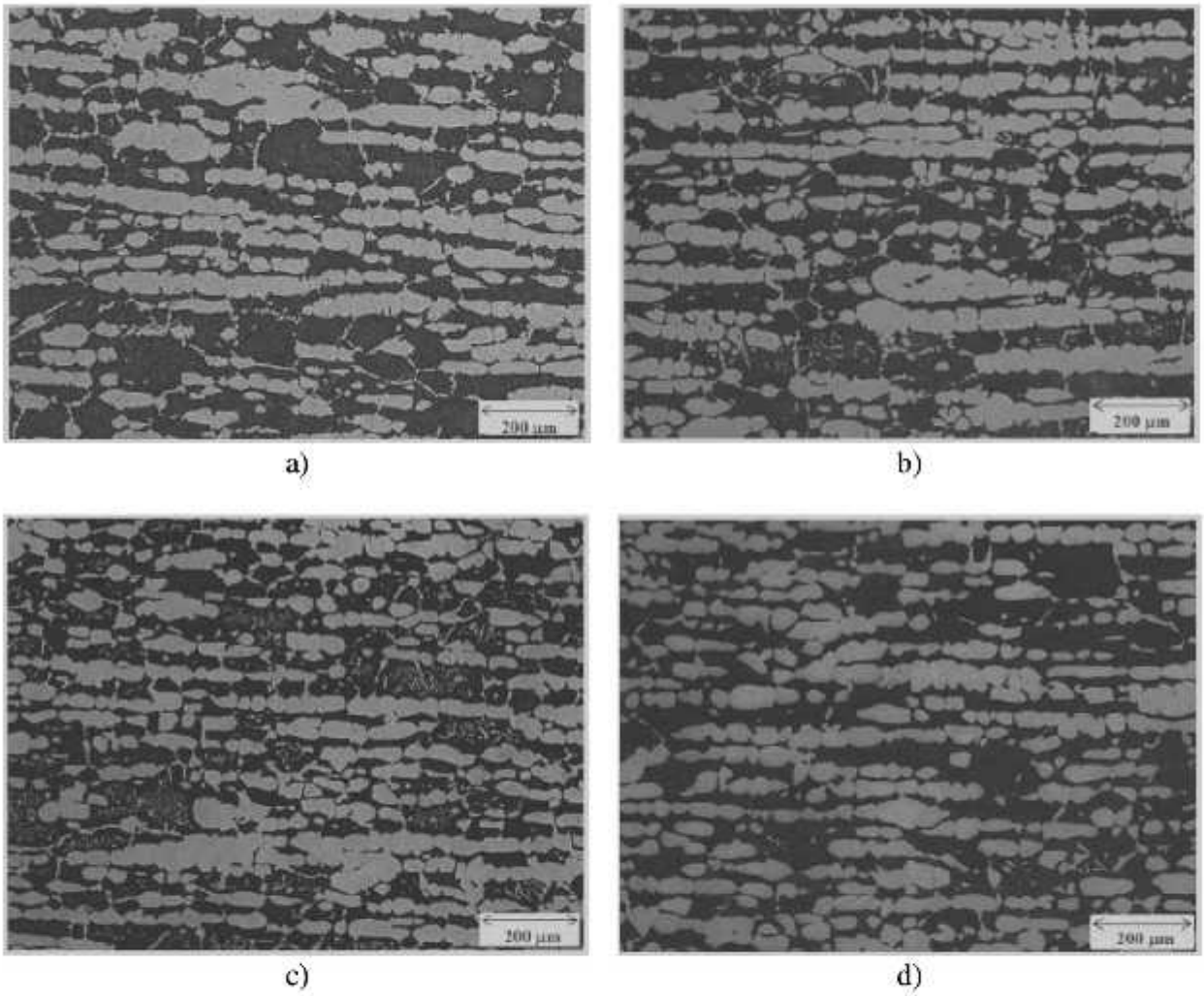

Fig. 4. Optical microscopy of the samples solubilized at 1088 °C for different times, etched with modified Beraha in a) 2 min, b) 30 min, c) 3 h and d) 36 h.

Chemical elements profiles at specific ageing times for both cycles and geometries of simulation were obtained as a function of the length model in DICTRA® simulations. Fig. 7 exemplifies the chromium profile at 1250 °C for the planar model.

Initial interface between ferrite and austenite can be seen in the composition profile associated to time zero of simulations at the horizontal distance of 10 µm. With the progress of simulation, during heating at 1250 °C, gradient profiles are developed at ferrite-austenite interface. Those composition profiles also indicate that the elements took longer to come into equilibrium in comparison with the phase's volume fraction. For the chromium profile in Fig. 7, attenuation of the composition gradient, which indicates full equilibrium, was only achieved after 10 hours at 1250 °C. Thus, if the material is thermally treated in only 30 min, time required for stabilization of the ferrite and austenite, there will still be a gradient of chemical composition and, consequently, heterogeneity of corrosion resistance along the phase extension, different from what is desired in practice, since there is a direct relation with PREN and pitting potential (EP). Regions with smaller PREN, like Cr- and Mo-depleted areas, will present reduced localized corrosion resistance [10-12], and this information can only be obtained with simulation in DICTRA®.

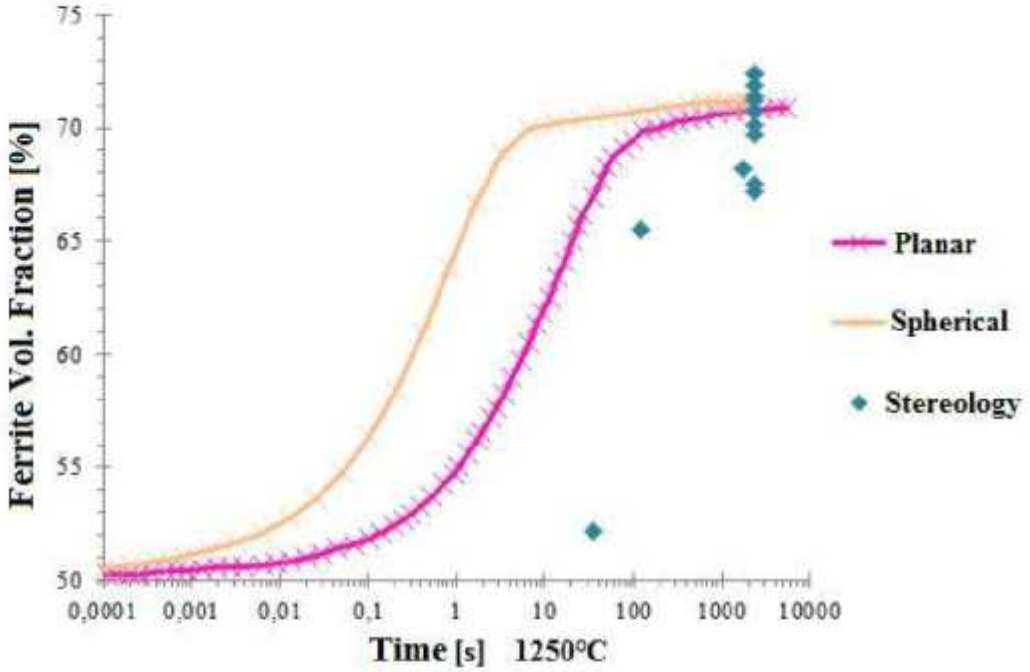

Fig. 5. Comparison between experimental results and simulation models of the ferritic phase volume fraction as a function of treatment time at 1250 °C.

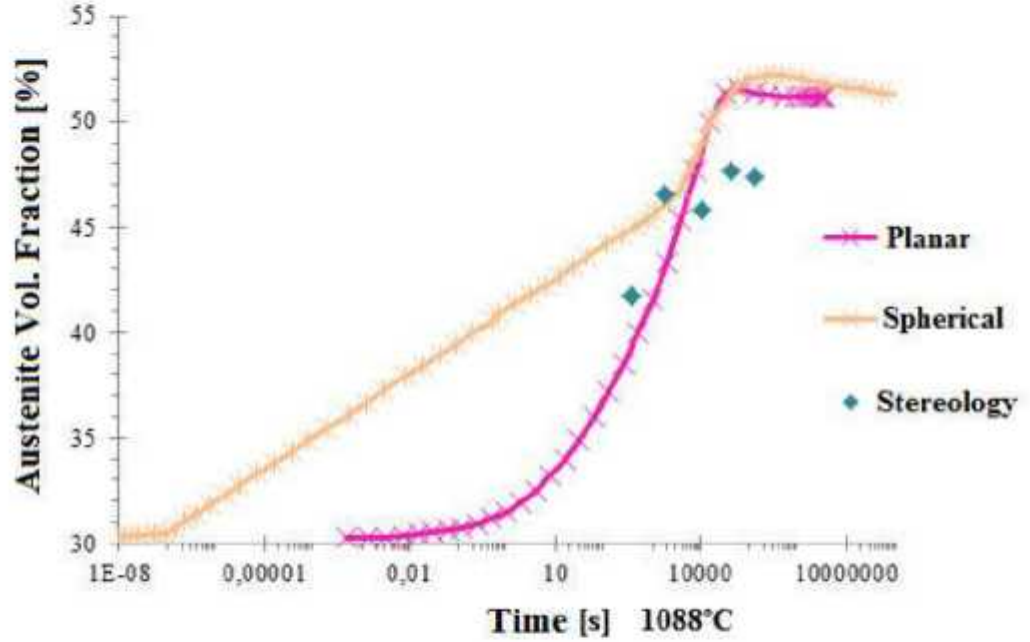

Fig. 6. Comparison between experimental results and simulation models of the austenitic phase volume fraction as a function of treatment time at 1088 °C.

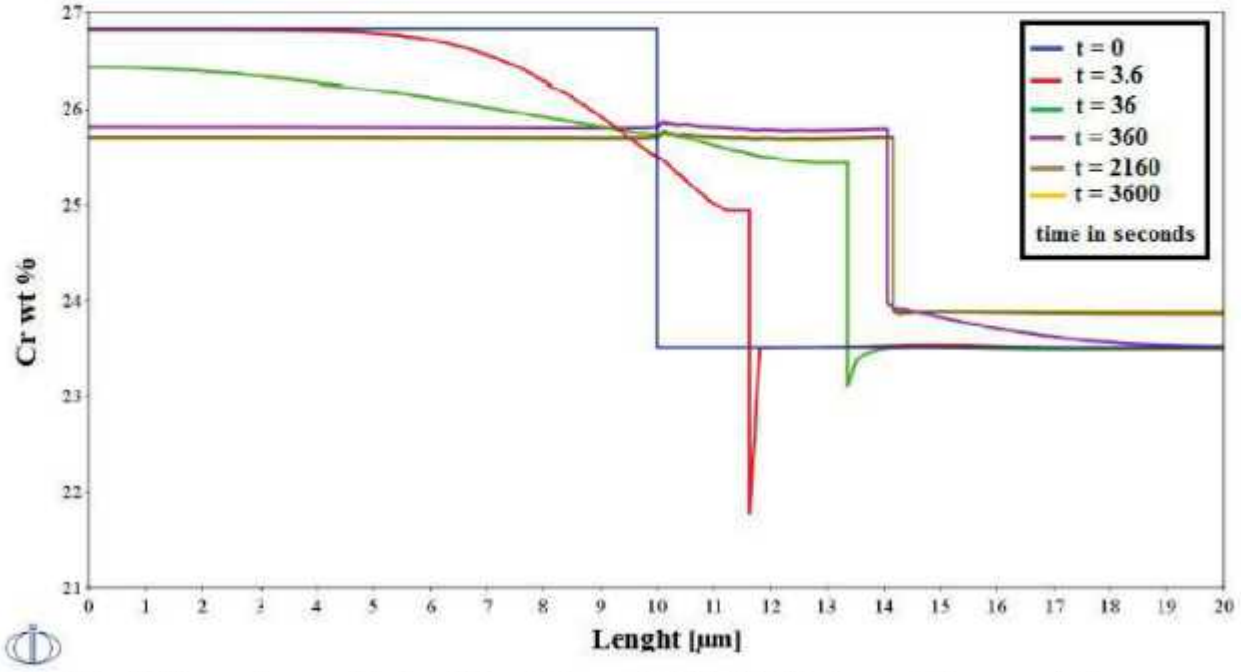

Fig. 7. Chromium profile in different times at 1250 °C obtained at planar model simulation.

5. Conclusions

1. None of the geometric models used in DICTRA® simulations was able to perfectly describe the changes in volume fraction of phases at forging or solution treatment conditions. However, planar model is the one that better assess the behaviour of volume fraction phase's changes for both heat treatments.

2. It is verified that the fractions of ferrite and austenite stabilize after 30 min of heat treatment, obtaining 71% of ferrite at 1250 °C and 51% of austenite at 1088 °C, and simulations results of volumetric fraction of phases are validated with those results.

3. Although the phases stabilize after 30 min, it is noticed that the equilibrium of chemical composition, marked as the absence of compositional gradients, is established long after the achievement of the equilibrium volume fraction of phases. The information about total attenuation of gradient profiles can only be obtained in DICTRA® simulations.

References

[1] H. D. Solomon; T. M. Devine, Dúplex Stainless Steel: A tale of two phases, Dúplex Stainless Steels, Ohio, Conference Proceedings, ASM Metals Park (1982) p. 693-756.
[2] E. C. Bain, W. E, Griffiths, An Introduction to the Iron-Chromium Nickel Alloys Trans, AIME, (1927, n.75), p.166-213.
[3] J.O. Nilsson, Mater. Sci. Technol. 8 (1992) 685.
[4] P. Paulraj, R. Garg, Effect of intermetallic phases on corrosion behavior and mechanical properties of duplex stainless steel and super-duplex stainless steel, Adv. Sci. Technol. Res. J. 9 (27) (2015) 87.

[5] H. Vannevik, et al., Effect of elemental partitioning on pitting resistance of high nitrogen duplex stainless steels, ISIJ Int. 36 (7) (1996) 807.
[6] G. V. Raynor; V. G. Rivlin, Phase equilibria in iron ternary alloys, London (1985.) p. 316-332.
[7] M. Fiorante, Validação Experimental dos Modelamentos Computacionais de Ciclos Térmicos de Solubilização de um Aço Inoxidável Superdúplex (2018), p. 16-24.
[8] D.A. Porter; K.E. Easterling, Phase transformations in metals and alloys, New York: Taylor & Francis (1992, 2ND Ed), p. 514.
[9] M. Avrami, Kinetics of phase change I, Journal of Chemical Physics (1939), p.1103-1112.
[10] R. Magnabosco, N. Alonso-Falleiros, Pit morphology and its relation to microstructure of 850 °C aged duplex stainless steel, Corrosion 61 (2) (2005) 130.
[11] N. Ebrahimi, et al., Correlation between critical pitting temperature and degree of sensitisation on alloy 2205 duplex stainless steel, Corrosion. Sci. 53 (2011) 637.
[12] R. Magnabosco, L. Morais, D. Santos, Use of composition profiles near sigma phase assessment of local corrosion resistance in a duplex stainless steel. Calphad-Computer Coupling Of Phase Diagrams And Thermochemistry, v. 64, p. 126-130, 2019.